JOURNAL OF PROPULSION AND POWER
Vol. 26, No. 3, May–June 2010

Role of Tip Clearance Flow in Rotating Instabilities and Nonsynchronous Vibrations

Huu Duc Vo*
École Polytechnique de Montréal, Montréal, Québec H3T 1J4, Canada

DOI: 10.2514/1.26709

Single- and multiple-blade-passage simulations of an isolated subsonic axial compressor rotor show that flow oscillations in the tip region, known as rotating instabilities and a driver for nonsynchronous vibrations, occur when only one of the two criteria for short-length-scale rotating stall inception is satisfied. This criterion is tip clearance backflow below the trailing-edge blade tip. The flow oscillations associated with rotating instabilities most likely result from impingement of this tip clearance backflow on the rear pressure side of the blade. This phenomenon could plausibly be modeled with an impinging jet subject to a lateral pressure gradient and lateral shear flow. The findings have important practical implications on the prediction and suppression of nonsynchronous vibrations.

Nomenclature

F	=	frequency
P	=	static pressure
Pt	=	stagnation pressure
U_{tip}	=	blade-tip speed (leading edge)
Vx	=	average inlet axial velocity
ρ	=	density
ϕ	=	flow coefficient, Vx/U_{tip}
ψ	=	total (stagnation)-to-static pressure-rise coefficient, $(P_{\text{out}} - Pt_{\text{in}})/0.5\rho_{\text{in}}U_{\text{tip}}^2$

I. Introduction

AS COMPETITION in the aerospace industry drives aircraft engines to become increasingly lighter through component weight reduction, vibrations that may not have been a concern in the past can become problematic. Traditional vibrations taken into account in the design of aeroengines blades are forced vibrations and flutter. Forced vibrations, which occur at blade-passing frequencies, refer to the vibrations caused by circumferential variations in the flowfield due to the wakes and potential effects of adjacent blade rows in relative motion. Flutter is a self-excited vibration from fluid–structure interaction that occurs at frequencies unrelated to blade passing. A yet-unexplained category of vibrations that is of increasing concern is nonsynchronous vibrations (NSVs), which can be strong enough to cause premature blade failure, as well as being a source of undesirable noise. They have been detected in the front stages of axial compressors and fans under stable operating conditions [1,2]. Although they also have frequencies unrelated to blade passing, NSVs differ from flutter in that they occur at operating parameters in which flutter is traditionally absent and may be driven by a fluid dynamic excitation source independent of blade vibrations [2].

Although a type of NSV linked to flow separation along the blade span of a fan stator has been recently reported [3], the majority of NSV cases studied so far seems to involve tip clearance flow unsteadiness, also known as rotating instabilities, in a fan or compressor rotor. In practice, the cases involving tip clearance flow should be much more common, as most modern blades are designed to minimize boundary-layer separation over operational flow ranges. Early experimental measurements on a multistage axial compressor by Baumgartner et al. [1] showed that the fluid dynamic instability associated with NSV is most pronounced in the rotor tip region. Experimental work by Liu et al. [4] and by Kameier and Neise [5,6] on an axial fan reported that rotating flow instability in the rotor tip region are the source of narrow frequency bands noise below the blade-passing frequency. Liu et al. [4] also differentiated these rotating flow instabilities from rotating stall. All of these authors [1,4,5] modeled the unsteady flow phenomenon as a fluctuating source rotating at a fraction of the rotor speed. Although the exact fluid dynamic mechanism of the source was not known, Kameier and Neise [5,6] reported that the rotating flow instability at the rotor tip only occurs when there is flow reversal in the tip clearance region, and that these instabilities are present for the larger tip clearance sizes and at flow rates equal to or lower than the design value. Later, combined experimental and numerical studies [2,7,8] point to tip clearance flow oscillations are the main source of flow unsteadiness behind nonsynchronous vibrations. Pressure measurements with transducers installed both on the casing and rotor blades by Mailach et al. [7] showed also that these flow oscillations occur at large rotor tip clearances and low mass flow, and that they grow in amplitude while slightly reducing in frequency as the mass flow is reduced along the pressure-rise characteristic (speed line) toward the stability limit (stall point). These authors attempted to explain the flow oscillations with fluctuating tip vortices. However, as mentioned in the corresponding discussion by Cumpsty [9] and concurrently observed in our work, it is hard to find a well-defined tip vortex at the low-mass-flow conditions near stall at which rotating instabilities usually occur. More recently, Fukano and Jang [10] carried out measurements with hot-wire probes rotating with a fan rotor. Their data for a plane just downstream of the trailing edge at the lowest experimental flow coefficient, which has not stalled, point to a region of large velocity fluctuations on the blade-tip pressure side. Unfortunately, the focus of this work was not on noise at lower than blade-passing frequency, associated with rotating instabilities, and the authors did not provide a more detailed study of the flowfield at this low flow coefficient. As things stand, a clearer explanation for the fluid dynamic origin of these flow oscillations and the parametric conditions for their occurrence are needed in order to eventually develop predictive capability and optimal suppression technologies for nonsynchronous vibrations. This is the objective of the present work.

Until now, most published studies have approached the problem with experimental measurements and multiple-blade-passage simulations of rotating instabilities and attempted to extract the physics from the unsteady flowfield. The present work approaches the problem from a different angle by starting out as a study of the formation of short-length-scale (spike) rotating stall disturbances [11]. The work is mainly based on time-accurate single-blade-

Presented as Paper 629 at the 44th AIAA Aerospace Sciences Meeting and Exhibit, Reno, NV, 9–12 January 2006; received 11 August 2006; revision received 26 February 2010; accepted for publication 3 November 2008.

*Assistant Professor, Department of Mechanical Engineering, 2900 Boulevard Édouard-Montpetit, 2500 Chemin de Polytechnique, Bureau C318.9. Member AIAA.

passage computations along the speed line up to the point of instability. In doing so, a link is made between the observed flow fluctuations and the criteria that set the formation of spike stall disturbances [11,12] that leads to a plausible hypothesis for the physics and prediction of rotating instabilities.

II. Computational Approach

The Reynolds-averaged Navier–Stokes computational fluid dynamics code UNSTREST by Denton [13] of the University of Cambridge was used for time-accurate single- and multiple-blade-passage flow simulations. It is a cell-centered code with a mixing-length turbulence model. The geometry simulated is an isolated GE E^3 rotor *B*, which forms the first rotor of a low-speed four-stage axial compressor with inlet guide vanes that has been tested at the General Electric Aerodynamic Research Laboratory [14]. The rotor has 54 blades with a solidity of 1.16, a stagger angle of 50 deg, and a hub-to-tip ratio of 0.85. The tip Mach number is approximately 0.2 with a Reynolds number based on blade chord of 300,000. However, the simulations were carried out at a tip Mach number of 0.5 to accelerate convergence. This geometry had been initially chosen for study because spike stall inception originating in this rotor had been measured [15].

The mesh used for each blade passage is $106 \times 41 \times 45$ with a pinched blade-tip model, as shown in Figs. 1 and 2. The blades do not vibrate in these simulations. A standard periodic boundary condition is applied to the circumferential edges of the computational domain. The upstream and downstream ducts have axial lengths of six blade pitches, allowing the mesh to be repeated circumferentially for simulations of up to six blade passages. Endwall shear stress is activated at a fixed short distance upstream of the leading edge to keep the incoming endwall boundary layer reasonably small. The inlet conditions consist of uniform stagnation pressure and temperature and axisymmetric incoming flow angles set to the spanwise distribution of inlet guide vanes exit flow angles. The exit boundary conditions consist of a specified casing static pressure and radial equilibrium. This exit casing pressure is incrementally increased at constant rotor speed to obtain converged flow solutions at different points along the pressure-rise characteristic (speed line). For small-to-medium tip clearances (1.8% chord and below), the solution converges to a constant mass flow and steady flowfield. For large tip clearances, especially at the lower flow coefficients, the converged solution shows periodic oscillations in mass flow, indicating an oscillatory flowfield.

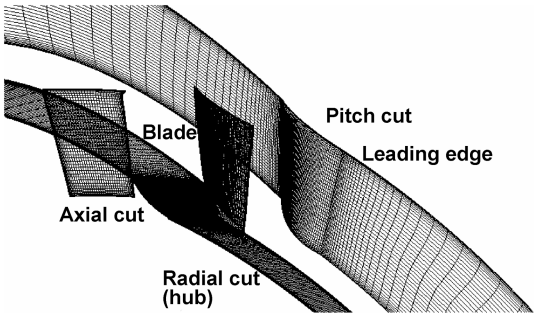

Fig. 1 Mesh for E^3 rotor *B* [11].

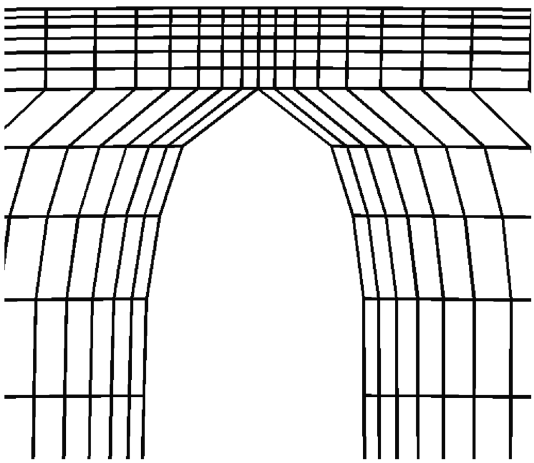

Fig. 2 Pinched blade-tip mesh.

For multiple (six)-blade-passage computations, the converged single-blade-passage solution is used as the initial condition. However, the combination of the code's cylindrical coordinates and axisymmetric inlet and exit boundary conditions causes the multiple-blade-passage solution to behave exactly as the single-passage solution. To remedy this situation, a very small inlet flow asymmetry is initially introduced through a temporarily applied full-span inlet stagnation-pressure perturbation of six blade pitches in wavelength and rotating with the rotor. The amplitude is selected to give a stagnation-pressure disturbance of about 0.2% of inlet dynamic head (based on rotor tip speed) at the rotor leading edge and lasting only 0.074 rotor revolution. This magnitude of nonuniformity is not unreasonable for practical applications. For cases with a fluctuating converged single-blade-passage solution, the mass flow of the six-blade-passage simulation initially oscillates at the frequency of the single-passage solution until about 1.5 rotor revolutions, when the oscillations shift to different frequencies as passage-to-passage flow asymmetry sets in.

III. Results and Discussion

Figure 3 shows the stagnation-to-static pressure-rise characteristics (speed lines) up to the stall point computed for the isolated E^3 rotor *B* at different tip clearances with time-accurate single-blade-passage computations.

Vo et al. [12] showed that the presence of two criteria will set the (rotating) stall inception point on a negative slope of the stagnation-to-static pressure-rise characteristic through the formation of short-length-scale (spike) stall disturbances in the rotor tip region. These disturbances rotate at a fraction of the rotor speed and grow rapidly into fully developed rotating stall. The two criteria are illustrated on a compressor rotor in Figs. 4a and 4b. Figure 4a depicts the backflow below the trailing-edge blade tip of tip clearance fluid from adjacent passages, impinging on the pressure surface below the blade tip. Figure 4b illustrates tip clearance flow leakage below the leading-edge blade tip. Reference [12] shows that the impinging flow in Fig. 4a has a tendency to move upstream due to the positive pressure gradient in the blade passage. However, when the interface between the incoming flow and (local) tip clearance flow is inside the blade passage (as in Fig. 4c), this impinging backflow is forced to either convect downstream or leak through the adjacent tip clearance. As the mass flow decreases, the incoming/tip clearance flow interface moves upstream [16]. When it reaches the leading-edge blade tip, as depicted in Fig. 4d, a path is opened at the leading edge for the tip clearance flow to leak through the adjacent blade passage, thus allowing impinging backflow to move upstream. This explains why both criteria must be satisfied for spike stall inception to occur. The findings from [12] are also independently supported by experiments on three low-speed single-stage axial compressors [17].

In Fig. 3, for the nominal case of 1.8% chord tip clearance, time-accurate simulations shows steady flow along the entire speed line with both criteria being met at about the same flow coefficient at the stall point. However, for larger tip clearances, such as the 3.0% chord tip clearance case which exhibits significant flow oscillations at the lower mass flows, trailing-edge backflow occurs at a higher flow coefficient (point 3) than leading-edge spillage (point 4). This is quantified in Fig. 5, in which point numbers correspond to those of Fig. 3. Figure 5a plots the time-averaged spanwise distribution of pitch-averaged mass flow, which becomes negative below the blade tip between points 3 and 4. However, according to Fig. 5b, the onset of tip clearance flow spillage below the blade-tip leading edge only occurs at point 4, which is the last stable point at the onset of spike stall inception. (Points beyond 4 are stall transient points.)

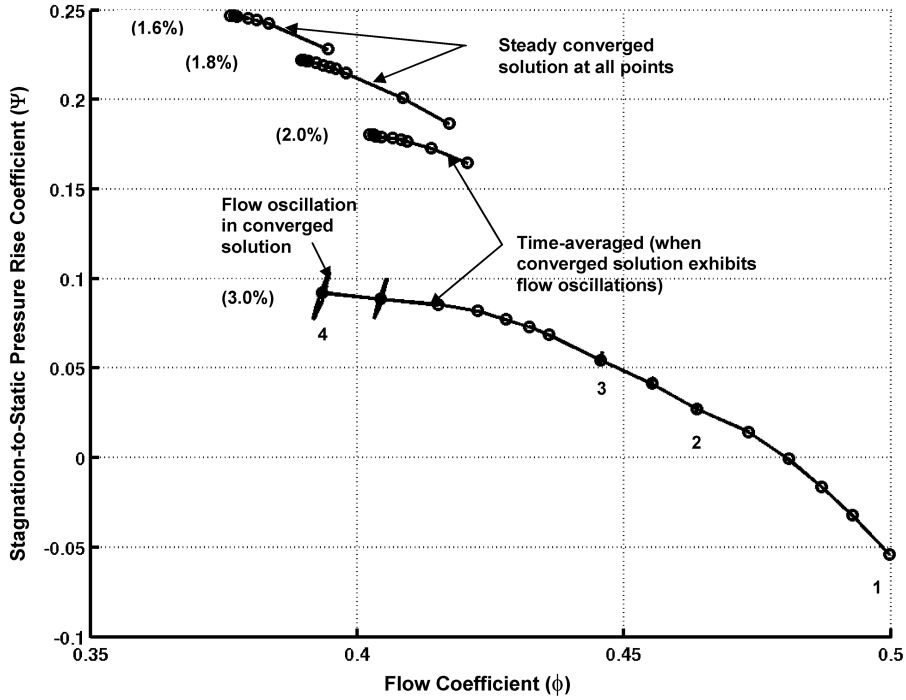

Fig. 3 Stagnation-to-static pressure-rise characteristic across E^3 rotor B at different tip clearances (% chord) from time-accurate single-blade-passage computations [11].

At flow coefficients between points 3 and 4, essentially the situation depicted in Fig. 4c, the flow exhibits periodic fluctuations. These oscillations are shown in Fig. 3 at 3.0% chord tip clearance by the instantaneous traces of stagnation-to-static pressure-rise characteristics for a few sample points for which the mass flow oscillations occur at only one frequency (points 2 through 3 and last two points before stall). Pressure traces reveal that the fluctuations are concentrated in the rotor tip region, as is the case for rotating instabilities. Figure 6 plots the power spectral density (PSD) for the converged mass flow oscillations (in the rotor frame of reference) for the 3.0% chord tip clearance case at different flow coefficients. The point numbers on the right correspond to those in Fig. 3. Two

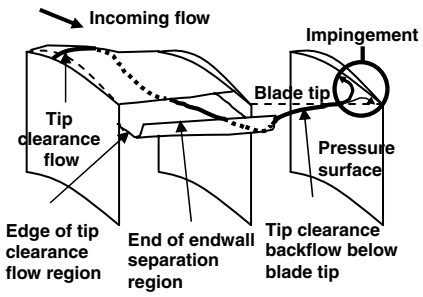

a) Trailing edge tip clearance backflow (spike stall criterion 1)

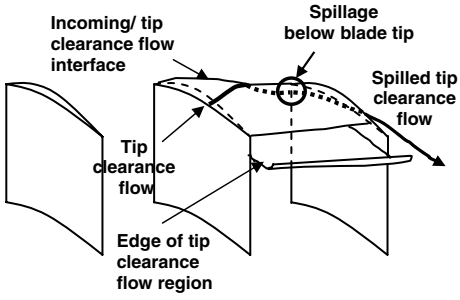

b) Leading edge tip clearance leakage (spike stall criterion 2)

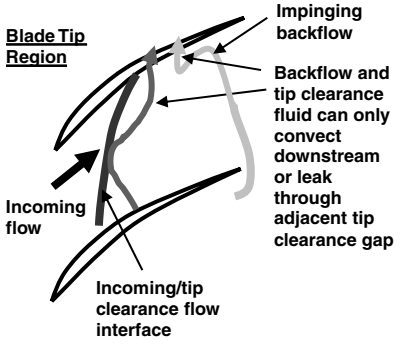

c) Backflow without spillage (only spike stall criterion 1 satisfied)

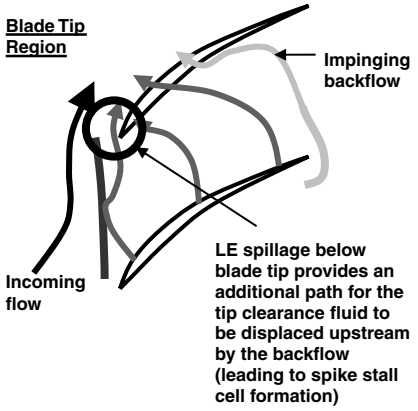

d) Backflow with spillage (both spike criteria satisfied)

Fig. 4 Criteria for formation of spike rotating stall disturbances [12] (LE denotes leading edge).

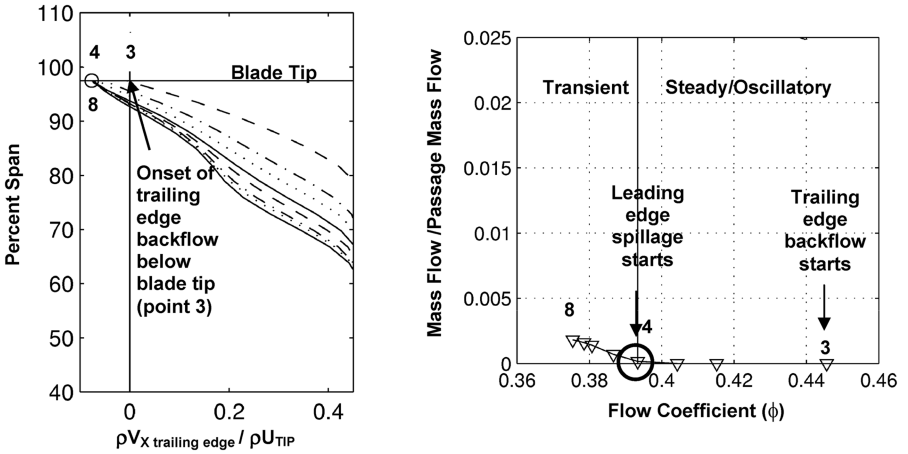

a) Spanwise distribution of pitch-averaged mass flow at passage exit plane (spike stall criterion 1)

b) Mass flow spilled ahead of leading edge below blade tip (spike stall criterion 2)

Fig. 5 Spike stall criteria evaluated for 3.0% chord tip clearance case [12].

important observations can be made. First, the dominant mode is at 0.35 rotor blade-passing frequency (BPF) for point 4 (highest oscillation amplitude). This frequency is in the range of the dominant frequencies associated with rotating instabilities as measured (in the rotor frame of reference) with strain-gauged or pressure sensors on rotor blades in [1] (∼0.18 BPF), [2] (∼0.36 BPF) and [7] (∼0.24 BPF). Second, the dominant mode's amplitude increases, while its frequency slightly decreases, with decreasing flow coefficient toward the stall point, just as reported in [7] for rotating instabilities. Furthermore, Fig. 6 also shows small oscillations at the dominant frequency at flow coefficients higher than that of point 3, which will be discussed later. However, the amplitude of these oscillations only undergoes a rapid increase with respect to decreasing flow coefficient after the onset of trailing-edge backflow below the blade tip at point 3.

Figure 7 presents the unsteady flow pattern, through static pressure contours at 96% span, at one time instant for a six-blade-passage simulation with 3.0% chord tip clearance at the inlet and exit conditions of point 4 in Fig. 3. Figure 8 presents the PSD of the pressure trace at the blade-tip span for the point indicated in Fig. 7 (leading edge, midblade pitch), moving with the rotor. The PSD in the rotor frame of reference, taken from traces over two rotor revolutions, looks very much like the blade vibration spectra for nonsynchronous vibrations in [1]. Although the dominant mode has shifted to about 0.25 BPF compared with single-blade-passage computations, the observed frequency is still in the range for measured rotating instabilities and NSV in the rotor frame of reference [1,2,7].

In summary, Figs. 6–8 showed that the observed converged flow oscillations in the single- and multiple-blade-passage simulations correspond to the rotating instabilities associated with nonsynchronous vibrations. According to Figs. 4–6, these vibrations grow significantly in the presence of trailing-edge tip clearance backflow below the blade tip causing impingement on the pressure side. This impingement is evidenced by comparing the relative flow vector and corresponding static pressure contours at 96% span (just below the blade tip) for the single-blade-passage time-averaged solutions at point 3 (onset of trailing-edge backflow, Fig. 9a) and point 4 (highest flow oscillation, Fig. 9b). Relative to point 3, point 4 has significant impinging flow as indicated by the associated characteristic concentric static pressure contours near the trailing-edge pressure side. This impingement pressure pattern can also be seen on several blade passages in Fig. 7.

It can thus be argued that the flow oscillations associated with rotating instabilities are the result of tip clearance flow impingement on the pressure side just below the blade tip. The oscillations

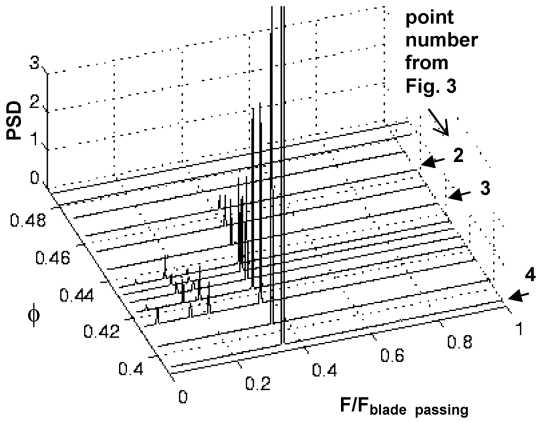

Fig. 6 PSD of mass flow oscillations for single-blade-passage computations at 3.0% chord tip clearance [11].

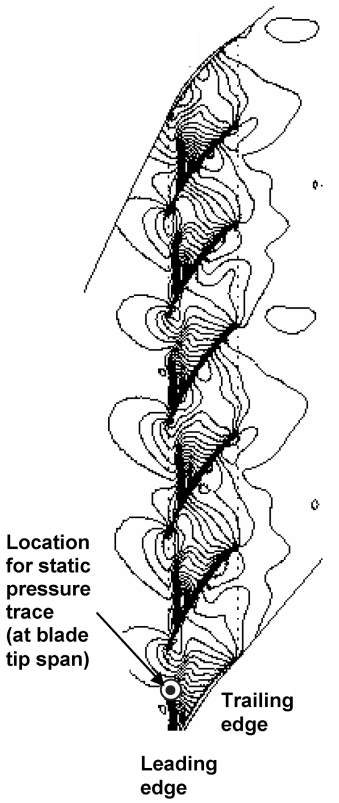

Fig. 7 Instantaneous static pressure contours at 96% span for six-blade-passage computation at point 4.

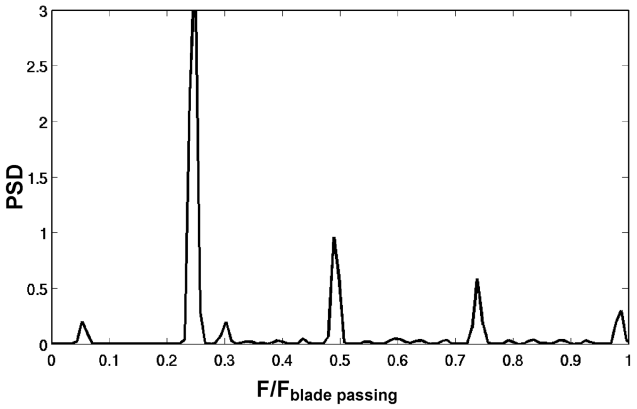

Fig. 8 PSD of static pressure trace (location shown in Fig. 7) for six-blade-passage computation at point 4.

themselves may be associated with the oscillatory flow dynamics of an impinging flow [18]. Thus, it could be possible to model rotating instabilities with a jet impinging on a plate in the presence of a lateral pressure gradient (that of the blade passage) and lateral shear in the opposite direction between the tip clearance and core flows.

Several additional observations further support the impinging flow hypothesis. First, Mailach et al. [7] reported that their rotating instabilities measurements on the rotor blades showed the disturbance to be more pronounced on the pressure side than the suction side of the blade, which is consistent with an impinging jet on the blade pressure surface. Second, the proposed impingement and its location (just below the trailing-edge blade tip) is further reinforced by hot-wire measurements by Fukano and Jang [10] on a plane just downstream of the rotor trailing edge that showed a region of high velocity fluctuations on the rotor pressure side near the tip at low mass flow. Third, hot-wire measurements near the casing downstream of the leading edge by Kameier and Neise [6], though not extending below the blade tip, showed flow reversal in the presence of rotating instabilities. If we can assume that this flow reversal trend continues to below the blade tip and toward the trailing edge, this would be consistent with the trailing-edge tip clearance backflow criterion leading to flow impingement, as illustrated in Fig. 4a. In fact, the tip clearance flow region delimited by the end wall flow envelop illustrated in Figs. 4a and 4b should be the same as the so-called secondary flow region referred to in [5,6]. Fourth, [6] also showed experimentally that the removal of flow reversal next to the casing, which according to our argument would prevent flow impingement, removed rotating instabilities. Last but not least, as mentioned earlier, small oscillations in mass flow were detected for converged solutions at flow coefficients between points 1 and 3 in Fig. 3, growing from negligible to noticeable amplitude at point 3, as shown in Fig. 6. All of this occurs in the absence of backflow below the trailing-edge blade tip. For these cases, the static pressure contours in Fig. 10 for points 1 (no flow oscillation at convergence) and 2 (small flow oscillations at convergence) of Figs. 3 and 6 indicate a small impingement pressure pattern on the pressure surface near the midchord for point 2, which is absent for point 1. Point 1 is a case with high flow coefficient (low blade loading), in which the tip clearance flow convects downstream without touching the adjacent blade. For point 2, with higher blade loading, the tip clearance flow has moved further upstream and its path has become more circumferential. As a result, there is an impingement induced by local tip clearance flow crossing the blade passage as opposed to by the backflow of tip clearance fluid from adjacent passages at the trailing edge. However, the observed flow impingement near midchord is much weaker, and the resulting flow oscillation amplitude much smaller (according to Fig. 6), than for the cases with trailing-edge tip clearance backflow.

Subsequent analytical and experimental research into impinging jets have been carried out to lend further support and quantitatively model the flow-impingement hypothesis. This work has led to a simple and promising model and equation involving resonance of an impinging jet on a flexible surface to predict the speed at which NSV occurs [19].

The findings described previously have two important practical implications. The first is the development of predictive capability for the occurrence, frequencies, and amplitudes of nonsynchronous vibrations. The above results point to the potential of widely used low-cost single-blade-passage computations, as done in this work, to predict rotating instabilities, mainly though the prediction of the occurrence of flow impingement. This type of simulation could then be combined with a model of flow oscillations associated an impinging jet, such as proposed in reference [19]. The resulting predictive tool would be of tremendous value to the gas turbine industry in the design of compressor and fan blades.

The second implication is the suppression of nonsynchronous vibrations. The above findings imply that any strategy that can remove trailing-edge backflow and/or flow impingement, will be successful in suppressing rotating instabilities and nonsynchronous vibrations. Examples include the addition of streamwise momentum to the tip clearance flow and/or the removal of tip clearance backflow through suction. The former effect has been empirically obtained by

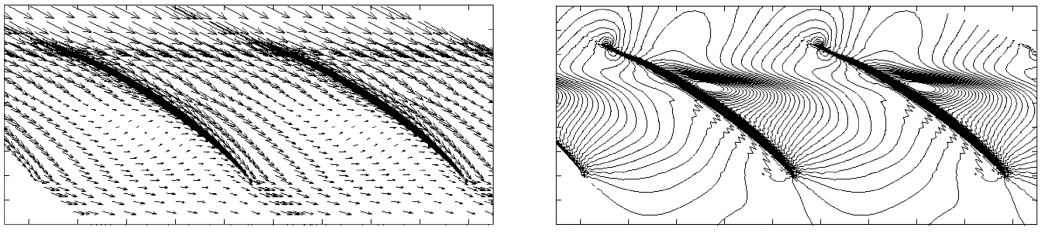

a) Relative flow vectors and static pressure contours at 96% span for point 3 in Fig. 3 (time-averaged single blade passage computation)

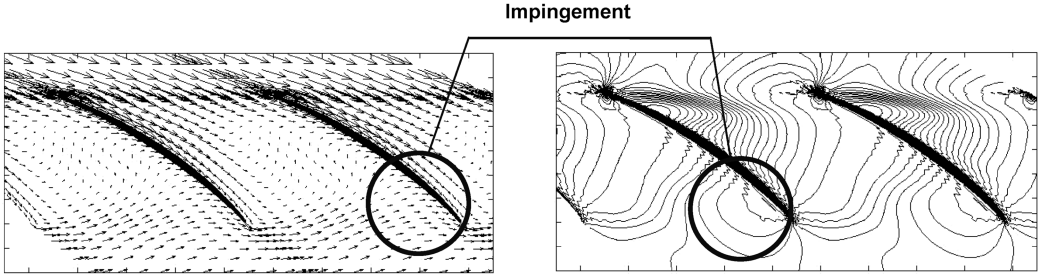

b) Relative flow vectors and static pressure contours at 96% span for point 4 in Fig. 3 (time-averaged single blade passage computations)

Fig. 9 Evidence of flow impingement from trailing-edge tip clearance backflow below the blade tip.

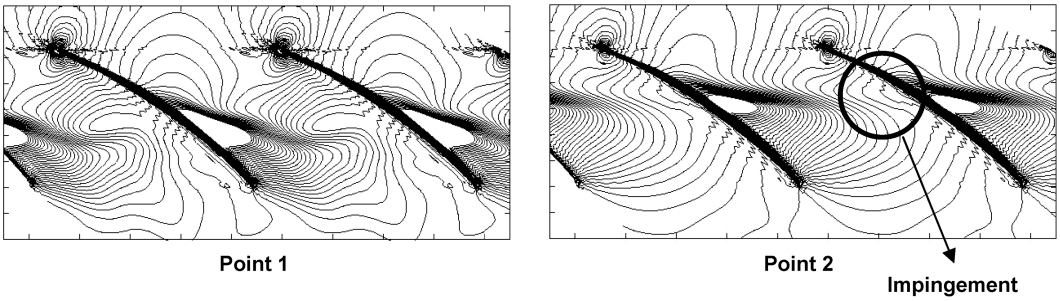

Fig. 10 Static pressure contours at 96% span for points 1 and 2 (time-averaged) in Fig. 3 (single-blade-passage computations).

Kameier and Neise [6] with the insertion of a turbulence generator in the tip clearance gap (which, in addition to partially impeding the tip clearance flow, presumably improved mixing of this low-momentum fluid with the high-momentum fluid of the core flow) and, more recently, by Neuhaus and Neise [20] using air injection at the casing, However, both effects should be achievable at the same time with well-designed casing treatments.

IV. Conclusions

Research into spike stall inception found the presence of rotating instabilities when only one of the two criteria for spike rotating stall inception is satisfied: namely, the backflow of tip clearance fluid from adjacent passages below the trailing-edge blade tip. This backflow leads to flow impingement on the pressure side of the blade near the trailing edge below the blade tip. The oscillatory flow behavior associated with impinging flows may explain the observed flow unsteadiness associated with rotating instabilities that drives nonsynchronous vibrations. At higher flow coefficients, where trailing-edge backflow is absent, small flow oscillations may arise from impingement induced by local tip clearance flow crossing the blade passage. Thus, rotating instabilities could plausibly be modeled by a jet impinging on a plate under lateral pressure gradient and shear from the core flow.

The above results imply that a practical low-cost predictive capability for rotating instabilities and nonsynchronous vibrations based on single-blade-passage computations, and an impinging flow model is possible if further research can assess the link between single- and multiple-passage oscillation amplitudes and frequencies and how these parameters are influenced by adjacent blade rows. In addition, the findings point to the removal of backflow and/or flow impingement as a successful strategy to suppress rotating instabilities and, by extension, nonsynchronous vibrations.

Acknowledgments

The author would like to thank J. D. Denton and L. Xu for their help in setting up the code and mesh and J. Thomassin for our discussions on the subject of nonsynchronous vibrations. Part of the data for this work were produced at the Massachusetts Institute of Technology's Gas Turbine Laboratory under the funding of the U.S. Air Force Office of Scientific Research, grant number F49620-00-1-0014, monitored by T. J. Beutner, whose support is gratefully acknowledged.

References

[1] Baumgartner, M., Kameier, F., and Hourmouziadis, J., "Non-Engine Order Blade Vibration in a High Pressure Compressor," International Symposium on Airbreathing Engines Paper 95-7094, 1995.

[2] Kielb, R. E., Thomas, J. P., Barter, J. W., and Hall, K. C., "Blade Excitation by Aerodynamic Instabilities – A Compressor Blade Study," American Society of Mechanical Engineers Paper GT-2003-38634, 2003.

[3] Sanders, A. J., "Nonsynchronous Vibration (NSV) due to a Flow-Induced Aerodynamic Instability in a Composite Fan Stator," *Journal of Turbomachinery*, Vol. 127, No. 2, 2005, pp. 412–421. doi:10.1115/1.1811091

[4] Liu, J. M., Holste, F., and Neise, W., "On the Azimuthal Mode Structure of Rotating Blade Flow Instabilities in Axial Turbomachines," AIAA Paper 96-1741, 1996.

[5] Kameier, F., and Neise, W., "Rotating Blade Flow Instability as a Source of Noise in Axial Turbomachines," *Journal of Sound and Vibration*, Vol. 203, No. 5, 1997, pp. 833–853. doi:10.1006/jsvi.1997.0902

[6] Kameier, F., and Neise, W., "Experimental Study of Tip Clearance Losses and Noise in Axial Turbomachines and Their Reduction," *Journal of Turbomachinery*, Vol. 119, No. 3, 1997, pp. 460–471. doi:10.1115/1.2841145

[7] Mailach, R., Lehmann, I., and Vogeler, K., "Rotating Instabilities in an Axial Compressor Originating from the Fluctuating Blade Tip Vortex," *Journal of Turbomachinery*, Vol. 123, No. 3, 2001, pp. 453–460. doi:10.1115/1.1370160

[8] Marz, J., Hah, C., and Neise, W., "An Experimental and Numerical Investigation into the Mechanisms of Rotating Instability," *Journal of Turbomachinery*, Vol. 124, No. 3, 2002, pp. 367–374. doi:10.1115/1.1460915

[9] Cumpsty, N. A., "Discussion: Rotating Instabilities in an Axial Compressor Originating from the Fluctuating Blade Tip Vortex," *Journal of Turbomachinery*, Vol. 123, No. 3, 2001, pp. 461–461. doi:10.1115/1.1371008

[10] Fukano, T., and Jang, C.-M., "Tip Clearance Noise of Axial Flow Fans Operating at Design and Off-Design Condition," *Journal of Sound and Vibration*, Vol. 275, Nos. 3–5, 2004, pp. 1027–1050. doi:10.1016/S0022-460X(03)00815-0

[11] Vo, H. D., "Role of Tip Clearance Flow on Axial Compressor Stability," Ph.D. Dissertation, Massachusetts Inst. of Technology, Cambridge, MA, 2001.

[12] Vo, .H. D., Tan, C. S., and Greitzer, E. M., "Criteria for Spike Initiated Rotating Stall," *Journal of Turbomachinery*, Vol. 130, No. 1, 2008, Paper 011023; also American Society of Mechanical Engineers, Paper GT2005-68374, 2005. doi:10.1115/1.2750674

[13] Denton, J. D., "The Use of a Distributed Body Force to Simulate Viscous Effects in 3D Flow Calculations," American Society of Mechanical Engineers Paper 86-GT-144, 1986.

[14] Wisler, D. C., "Core Compressor Exit Stage Study," Vol. 4, NASA Lewis Research Center, CR-165357, Cleveland, OH, 1981.

[15] Silkowski, P. D., "Measurements of Rotor Stalling in a Matched and Mismatched Multistage Compressor," Massachusetts Inst. of Technology, Rept. 221, Cambridge, MA, April 1995.

[16] Koch, C. C., "Discussion of Benser W. A.: Transonic Compressor Technology Advancements," *Fluid Mechanics, Acoustics, and Design of Turbomachinery, Part II*, SP-304, NASA, 1974.

[17] Deppe, A., Saathoff, H., and Stark, U., "Discussion: 'Criteria for Spike Initiated Rotating Stall'," *Journal of Turbomachinery*, Vol. 130, No. 1March 2005, Paper 015501. doi:10.1115/1.2750673

[18] Ho, C.-M., and Nosseir, N. S., "Dynamics of an Impinging Jet. Part 1. The Feedback Phenomenon," *Journal of Fluid Mechanics*, Vol. 105, 1981, pp. 119–142.

[19] Thomassin, J., Vo, H. D., and Mureithi, N. W., "Blade Tip Clearance Flow and Compressor Nonsynchronous Vibrations: The Jet Core Feedback Theory as the Coupling Mechanism," *Journal of Turbomachinery*, Vol. 131, No. 1, 2009, Paper 011013; also American Society of Mechanical Engineers, Paper GT2007-27286, Montreal, Canada, 2007. doi:10.1115/1.2812979

[20] Neuhaus, L., and Neise, W., "Active Control to Improve the Aerodynamic Performance and Reduce the Tip Clearance Noise of Axial Turbomachines," AIAA Paper 2005-3073, 2005.

C. Tan
Associate Editor